

PAPER • OPEN ACCESS

Experimental verification of the parameters affecting the characteristics of mechanical and corrosion behaviour of conventional and high-speed remote scanner laser welding of stainless-steel joints

To cite this article: Ahmed. M. El-Aziz *et al* 2019 *IOP Conf. Ser.: Mater. Sci. Eng.* **610** 012008

View the [article online](#) for updates and enhancements.

A promotional banner for the ECS 240th Meeting. The banner features a colorful striped border at the top. On the left, the ECS logo is displayed in a green circle. To the right of the logo, the text reads: "240th ECS Meeting", "Digital Meeting, Oct 10-14, 2021", "We are going fully digital!", "Attendees register for free!", and "REGISTER NOW" in bold orange letters. On the right side of the banner, there is a photograph of a diverse group of people in a professional setting, with a man in a white shirt and tie clapping and smiling.

ECS **240th ECS Meeting**
Digital Meeting, Oct 10-14, 2021
We are going fully digital!
Attendees register for free!
REGISTER NOW

Experimental verification of the parameters affecting the characteristics of mechanical and corrosion behaviour of conventional and high-speed remote scanner laser welding of stainless-steel joints

Ahmed .M. El-Aziz¹, Mahmoud Abou El Khier^{1,3}, Horest Exner²

¹German University in Cairo, Materials Engineering Department, 11835 New Cairo, Egypt

²Hochschule Mittweida (FH), Technikumplatz 17, D-09648 Mittweida, Germany

³ E mail. mahmoud.abuelkhier@gmail.com

Abstract. Nowadays technologies have huge assortment of welding processes are available and used in joining metals. The characteristics of the microstructures through weld zones, Scanning electron Microscope investigated the grain size before and after weld with the precipitates and the size and the extent of heat-affected zones (HAZ) will primary depend on: (1) the type of metals being joined, (2) the heat treatability of the material and welding velocity, (3) the classes of welding or joining processes used. The microstructure changes arising from welding will significantly affect the mechanical and the corrosion behaviour of the welded stainless steel. Because of lack of information which welding processes are the best method and the contradictory opinions regarding efficiency of different welding techniques. Accordingly, the present study has been undertaken to evaluate the mechanical and corrosion behaviour using different welding techniques, laser welding and conventional welding. Two welding techniques for Standard Austenitic stainless steel **1.4301(304)** are presenting in this study: Case (I) gas tungsten arc welding (GTAW) or TIG; Case (II) High-speed remote scanner laser-welding.

Keywords. Welding parameters, 1.4301(304) microstructure, hardness, Ferrite %, corrosion behaviour of laser and conventional welding, Open circuit potential (OCP), Potential cyclic voltammetry (PCV), energy-dispersive X-ray (EDX), Scanning electron microscope (SEM).

1. Introduction

Due to high demand on stainless steel in industrial application and welding of complex shapes is necessary. One of the challenges in conventional welding Tungsten inert gas(TIG) is the change in the composition of the material due to high heat distortion welding that the Remote Scanner Laser welding is used extensively due to its small and narrow welding zone. Due to narrow focusing zone of the laser beam, a very low heat input is produced in the weld bead which in turn creates no HAZ or a very narrow HAZ. Moreover, the less residual stress is produced in the weld metal and the less deformation is produced in the weld bead [1]. The selection of filler metals, fixtures and equipments, along with suitable preparation of samples and welding parameters can lead to creation of a sound joint.

1.4301 (304) the Austenitic stainless steel is one of the most common types of stainless steel on its list. It has microstructures that include Nickel, Molybdenum and Chromium. The structure of austenitic



stainless steel is the same as what you would find in regular steel. But only in a much higher temperature (up to 1200°C [2192°F]), giving it formability and weld ability. Furthermore, you can make austenitic stainless steel corrosion resistant by adding Chromium, and Molybdenum. As it contains Ni,Cr at conventional welding temperatures 200°C to 300°C might form carbide precipitates at grain boundaries thus intergranular corrosion will be produced. Austenitic stainless steel has the useful property of retaining a helpful level of toughness and ductility when welded to have high strength. Typical austenitic stainless steel is susceptible to stress corrosion cracking, but austenitic stainless steel with higher nickel content has increased resistance to stress corrosion cracking. Nominally non-magnetic, austenitic stainless steel shows some magnetic response depending on its composition. [2,3]

High speed remote scanner laser fig.1 welding on large thicknesses is a generally new topic; so it is essential that high penetration is made inside these thick-nesses with least distortion to acquire optimum results [4]. Laser beam welding gives Weldment least distortion and minimum heat-affected zones compared to conventional tungsten inert gas (TIG) welding which offers a solution for welding critical joints, and for situations where small or exceptionally precise welds are required it produces a high-quality and high-purity weld compared with other joining processes, which is crucial in many applications. Keyhole welding or deep penetration welding is a procedure in which the laser beam penetrates partially or completely through a specimen forming a keyhole; so as the laser beam progresses fig.2, molten metal fills in behind the hole to form the weld bead; which results in a homogenous weld. At the point when high laser beam power densities are accomplished, deep- penetration fusion welding is cultivated by a keyhole energy transfer mechanism. The price of TIG welding services is also usually quite affordable; but the process has a low deposition rate and if performed improperly, inclusions, contaminations, and unbalanced heating can cause products to become warped or defective [5][6]. In the auto-motive industry the laser technology was implemented to increase the productivity, strength of constructions and new designs [7,8]. First applications with long welds on the vehicle body are currently trailed by replacement of resistive spot welds by short laser welded fastens with the benefit of shorter preparing times.



Figure 1 Working area of laser scanner system
(Courtesy of trumpf laser technique) [11]

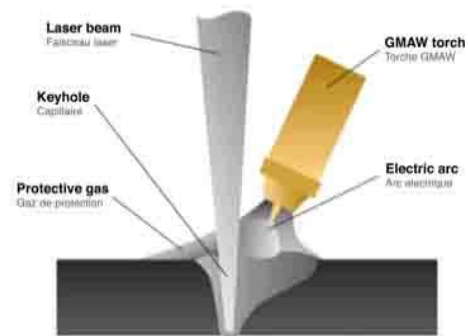


Figure 2 Key hole penetration between
Laser and TIG

In the present study the mechanical and corrosion properties of austenitic stainless steel (304L) welded laser was characterized in comparing with Tig as conventional welding. The challenges in welding stainless steel can be solved by using Remote scanner laser due to less heat distortion and effects on HAZ as the speed of laser is significant effect on the characteristics of HAZ where in less precipitates of carbide as ferrite are formed with high speed. In this study the mechanical test used in Micro hardness, Ferrite content, Tension tests. followed by corrosion test by open circuit potential (OCP) and potential cyclic voltammetry The mechanical properties and corrosion resistance of laser-welded stainless steels and conventional tungsten inert gas welded stainless steel may be deteriorated due to micro-segregation which attacked during the corrosion test due to the weld zone, presence of porosities, unfavorable phase

content, micro-fissures, solidification cracking and loss of materials by vaporization. So, to see the effect of these microstructure changes on the material.[9,10]

2. Experimental procedure

The chemical Composition of the Stainless Steel shown in the table 1 1.4301 (304) standard austenitic stainless steel (A.S.S)[12]

Table 1. Chemical composition (wt. %) of the Stainless steel 1.4301 (304) used in the study.

Code		C	Si	Mn	P	S	Cr	Mo	Ni	Cu	N
DIN	AISI										
1.4301	304	≤0.07	≤1.0	≤2.0	≤0.035	≤0.015	21.0- 23.0	2.50- 3.50	4.50- 6.50	-	0.10- 0.22

2.1. Material preparation

The materials received as 400 mm x 100 mm plates; so to create work-pieces of suitable dimensions, they had to be cut carefully so as not to change the metallurgical structure of the materials. A suitable cut-off wheel (50A25 cut-off wheels) was used during water-cooling to prevent changes in metallurgical structure and the sheets were clamped mechanically to provide a straight edge suitable for welding.

For the tensile tests, 100 mm x 25 mm pieces were cut and the welding edges were prepared by cutting off the rough edges to provide us with suitable edges which help in providing deep welding penetration and minimum distortion. After preparing these pieces, welding was done to provide us pieces with approximately 200 mm x 25 mm dimensions. For Stainless steel 1.4301 8mm thickness 4 welded specimens (2 remote scanner laser welding and 2 Tungsten inert gas welding), 2 un-welded specimens were tested for comparison.

The welding of Stainless steel 1.4301 sheets of such large thicknesses 8mm was a dubious technique; literature was not useful in giving us exact weld speed to perform an exceptionally solid weld. In this way, we took the recommended weld speeds from references, and after a few preliminaries, we utilized a weld speed that gave us a weld that looked sound upon visual inspection.

The welding equipment used a high-power about 3kW (Ytterbium Fiber Remote Scanner Laser), the shielding gas used was Argon. The materials were clamped in place mechanically to reduce thermal distortion of the material due to welding. No filler metals were used. Therefore, to guarantee that we obtain high-quality welds in high thicknesses, the welding was done by keyhole welding technique.

For Tungsten inert gas welding (TIG) equipment with high power 3KW and a direct current (DC) of 80 ampere with a shielding gas of pure Argon at pressure of 5 Bar which is flowed also to remove atmospheric contamination and protect the filler metal with the weld zone from impurities. There is only one type of weld used for the 1.4301 stainless steel with process of counter welding and inside with using a filler metal Microstructure: Austenite with 7-9% ferrite. Typical ferrite number is 6 Flux Color: White-Grey; with a chemical analysis table 2[13]

Table 2. TIG filler metal chemical analysis

C	Mn	Si	S	P	Cr	Ni	Mo	Cu	Fe
0.018	0.9	0.75	0.01	0.02	0.19	0.12	2.65	0.1	Balance

The welding speeds for Stainless Steel 1.4301 for thickness 8mm as follow:

- i) Remote Scanner laser Parameters :2.5m/min
- ii) Tungsten inert gas (TIG) parameters :8mm/min

2.2. Microstructure investigation

The laser-welded and Tig welded specimens were sectioned, polished and etched. The microstructure and phases in the weld line were analysed by Zeiss Axioscope 7 optical microscopy. The weld defects inside the weld profile were also examined to determine if improvements can be made inside the weld

in the future which will minimize weld defects, such as incomplete penetration, porosity and cracking. Also the size of the grains changed from the base metal to the heat affected zone (HAZ) to the weld zone which totally different for the types of weld (Laser-Tig). Using EVO-MA15 for Scanning electron microscope (SEM) to give more detailed information about grain size and behaviour in weld zone, energy-dispersive X-ray (EDX) to trace the important elements.,

2.3. Mechanical testing

I Micro hardness test

The Vickers micro hardness was used to attain the hardness of the specimens across line path according to (ASTM E384-99), [14] standard done through the top and side surfaces of the specimen of the laser-welded specimens and the Tig welded specimens as shown in fig.3 The load applied was 300 g and the loading time was 15 s by equipment Buehler Micromet 5100 series. All the specimens were ground to provide a smooth surface for the test.

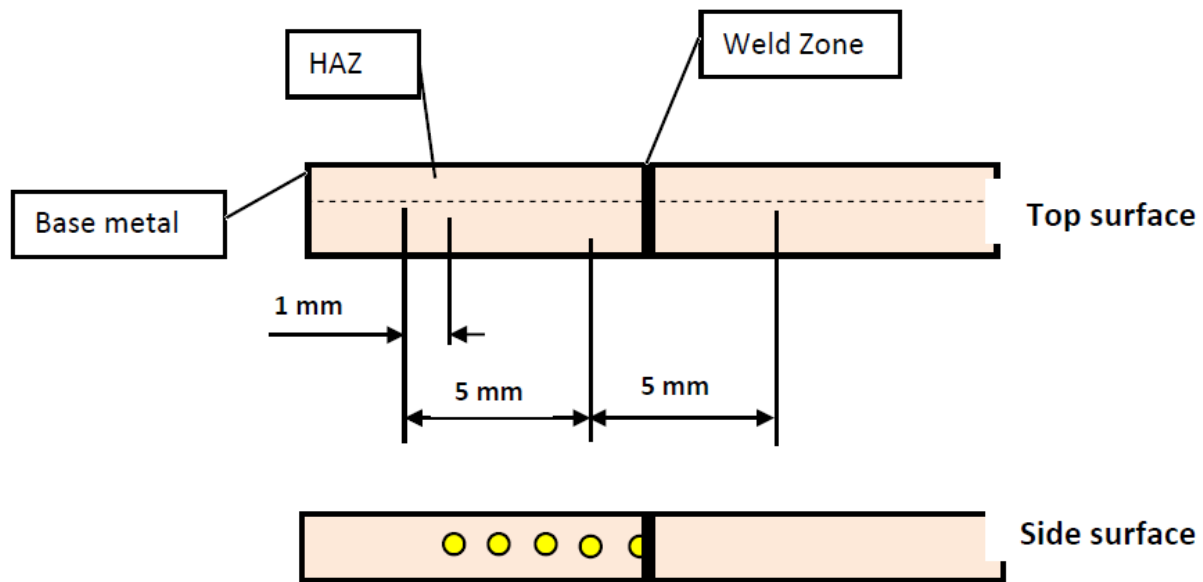


Figure 3 Schematic for specimen shown Base metal-HAZ-Weld zone

ii. Tensile test

Tensile tests on welded and unwelded specimens were performed to observe the mechanical performance of the welded specimens by equipment zwick Roell Z100. The observed property in this test was the Ultimate Tensile Strength [15]. To obtain the geometry that was according to ASTM E8 Standard [16] the material was machined using CNC machining. The tensile test was carried out at Strain rate from 0% to failure = 5 mm/min.

iii. Ferrite content

Ferrite testing is accurate way to measure delta ferrite content in austenitic. When ferrite content is too high, stainless steel can lose ductility, toughness, and corrosion resistance – especially at high temperatures. If ferrite content is too low, stainless steel welds become susceptible to hot cracking or solidification cracks.

For 1.4301 standard Austenitic stainless-steel specimen is well prepared surface after grinding and smooth polishing passing with the indenter probing through all the specimen starting with the base metal moving to the heat affected zone followed by the weld zone same on the other side of the weld zone to complete the path pattern through the top and side surface of the specimen. By equipment Fischer MP30 Feritscope by moving speed 0.5mm according to ASTM A799 / A799M [17]

2.4. Corrosion behaviour

Electrochemical test done several number of experiments done that is related to stainless steel Weldment, to examine the effects of such high-speed welding and tungsten inert gas welding on the corrosion behaviour of the Stainless steel 1.4301 [18]. The instrument used was a PGZ-100 Volta lab potentiostat. The specimen is covered with an epoxy cold mounted and left to harden. After removing from the mould, the specimen are ground using (180-1200) SiC wet grinding paper, then polished up to 1 μm and finally dried and become ready for the test [19,20]. Electrochemical measurements of the base metal and the welded materials (Laser welded-Tig welded) was carried out in 3.5% NaCl solution, all potentials are measured relative to a saturated calomel electrode (SCE) at 25°C.

- Open-circuit potential (OCP) for every specimen, the OCP was performed for 90 minutes.
- Potential cyclic voltammetry (PCV) is performed (-300 to 700) mV below the OCP of the material until a suitable voltage with a scan rate of 2 mV/s for 1 Cycle.
- The corrosion rate is obtained using the Tafel method.

3. Results and discussion:

3.1. Optical microscope results:

Weld defects:

It is observed that there is different types of defects where detected happen from welding as shown in fig.4 and fig.5 for laser welded and Tig welded specimens respectively. The most common defect observed is complete penetration and under fill of the weld bead due to the reflection of the incoming laser off the surface of the stainless steel same for the Tig happened due to the filler rod melting. A solution to decrease the defects so decreasing the reflectivity of the laser off the surface of the material. It can be coating of the surface to absorb and decrease the surface reflection. [21]

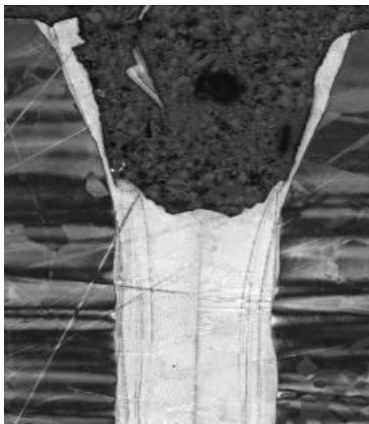


Figure 4. 1.4301 Laser weld under fill

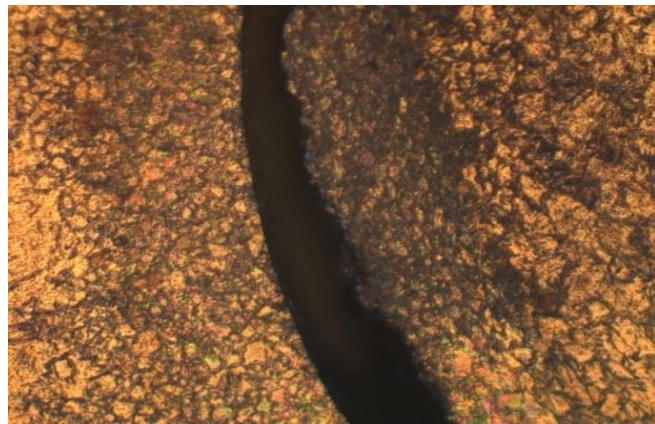


Figure 5. 1.4301 8mm Tig weld under fill

Microstructure investigation:

Observed from optical microscope that the grain size in the base metal and HAZ its much bigger before deformation than the weld zone that gives smaller grain size and hardened the stainless steel. Elongation through grains is shown in the different zones in the weld towards the HAZ. The carbide precipitates seen clearly due to the high temperature of welding which caused the sensitized stainless steel [22,23]. As shown in fig.6,7 for Tig weld compared to the laser weld fig.8,9.

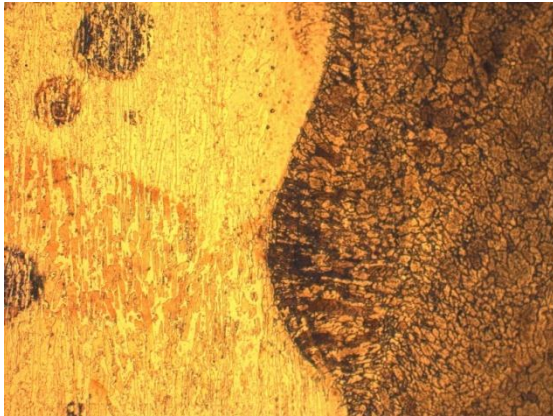


Figure 6. 1,4301 TIG weld

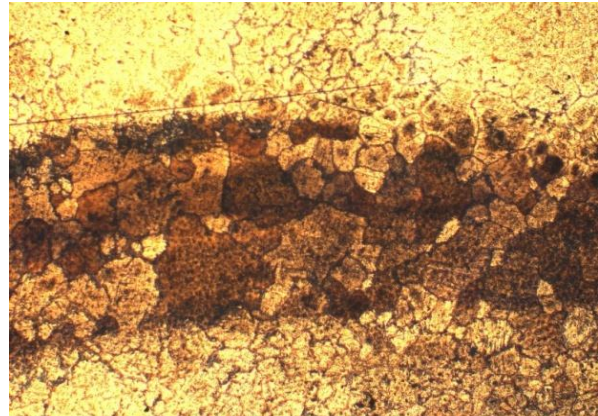


Figure 7. 1,4301 TIG weld



Figure 8. 1,4301 Laser weld

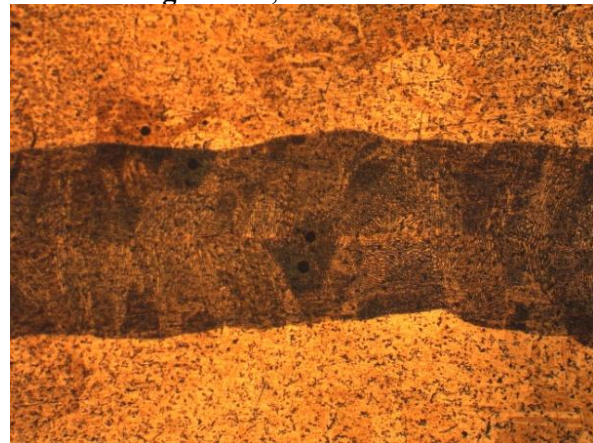


Figure 9. 1,4301 TIG weld

3.2. *Scanning electron microscope (SEM)*

SEM is done to observe further information about grains behavior in the weld zone figs 10-12

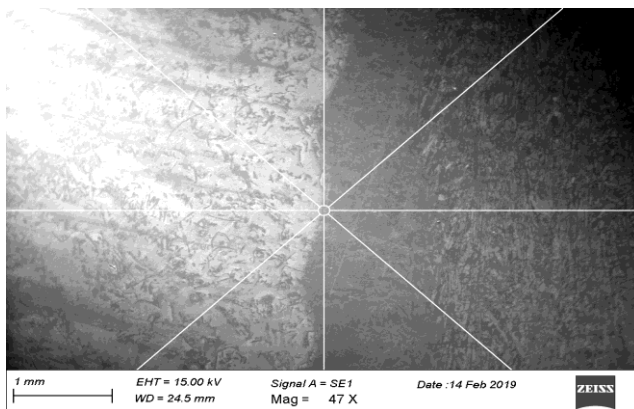


Figure 10. 1,4301 A.S.S SEM weld zone TIG weld

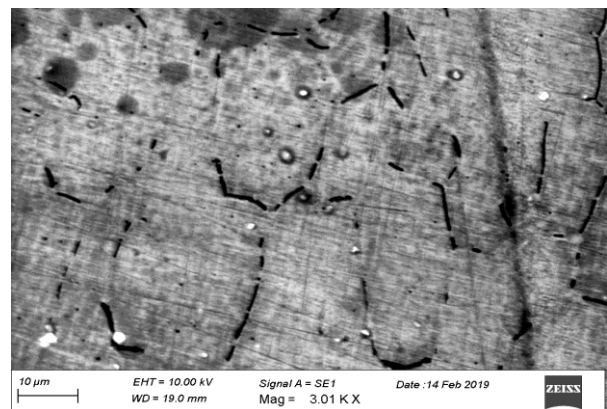


Figure 11. 1,4301 A.S.S SEM HAZ at TIG weld line

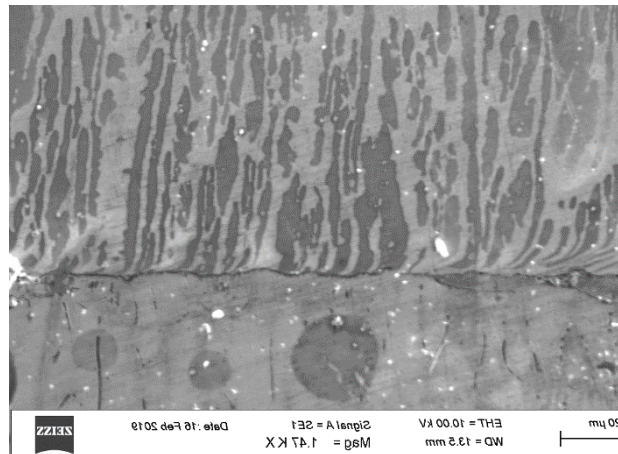


Figure 12. 1,4301 A.S.S SEM Weld zone at LASER weld

After Scanning electron microscope observed more investigation about the grains behaviour inside the weld zone and HAZ. there is a difference. The grain size of this material was very clear in figure 10,12 by the help of magnification we can see its very small and may be this explains why the hardness at this region is higher. doubting that these black spots are carbides figure 11 but after making the EDX table 3 and comparing between the HAZ and base metal or even though change in percentage of the iron or chromium so this means that there is no precipitation and the heat generated from the remote scanner welding just make recrystallization of the grains. also the heat affected zone has a lot of grain orientations which will the properties of the material according to the direction of the grains.

3.3. Energy-dispersive X-ray(EDX)

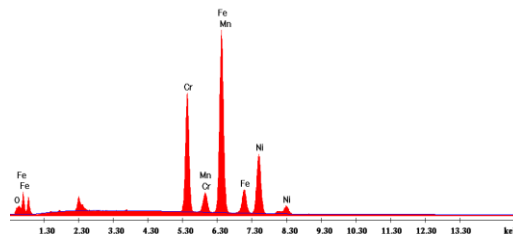


Figure 13- EDX 1.4301 A.S.S at HAZ Laser weld

Table 3. As explained in fig.13, of Energy-dispersive x-ray (EDX) that :

Element	Wt%	At%	K-ratio	Z	A	F
O k	2.02	6.71	0.0082	1.1371	0.3534	1.0036
Cr k	21.24	21.65	0.2379	0.9882	0.9807	1.1557
Mn k	1.25	1.21	0.0125	0.9721	0.9920	1.0352
Fe k	50.23	47.66	0.4880	0.9925	0.9373	1.0441
Ni k	25.25	22.78	0.2191	1.0127	0.8572	1.0000
Total	100.00	100.00				

3.4. Micro hardness test:

After performing hardness testing on the work pieces, it is a general pattern that the hardness increments towards the weld line until it is at its maximum at the centre at the weld zone going from the base metal to HAZ then to weld-zone, as found in figures (14 and 17) for top surfaces, figure (14 and 15) for side surfaces. The phenomenon might be clarified by a purpose behind stainless steel 1.4301. The main reason may be because of the grain refinement and the formation of smaller grains as in the small grain, no dislocation can travel more than 1 Unit of distance. This type of strengthening is known as Hall-Patch strengthening. which implies more grain boundaries. These grain boundaries give more strength to the material which causes an increase of the hardness. For Austenitic stainless steel 1.4301 (304) the hardness for the welded specimens were much higher than the unwelded. There is a great increase in the TIG weld over the laser weld compared to the unwelded.

Since, a very large increase in the ferrite is observed, where the primary phase becomes the ferrite phase, so a very large increase in the hardness is observed reaching as much as 54% more than the original hardness as seen in Figure 17. comparing to literature result for the unwelded sample which is 200 HV close to the result in figure 18. Which is 197 HV compared to the welded samples higher than the unwelded.

Hardness on top surface:

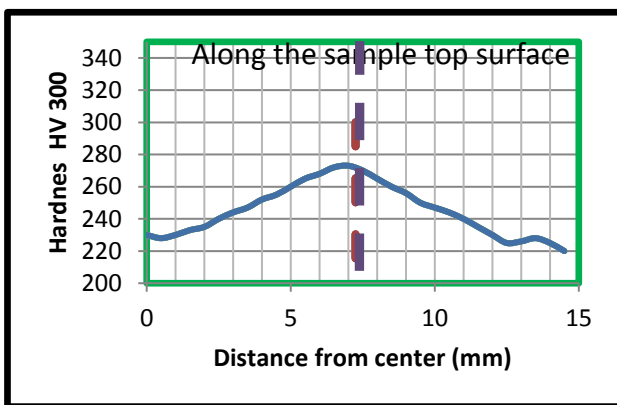


Figure 14- 1.4301 A.S.S top surface Laser weld hardness chart

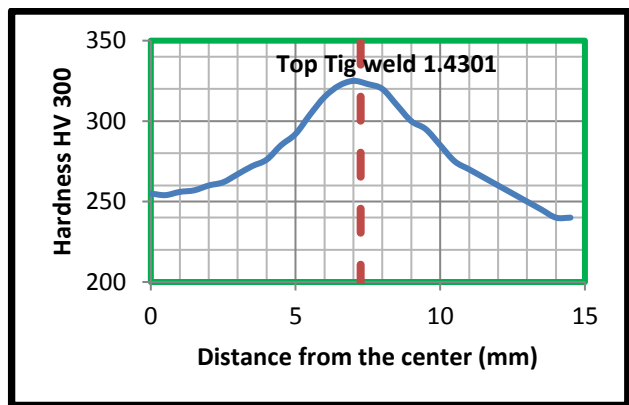


Figure 15-1.4301 Top surface A.S.S TIG weld hardness chart

Hardness on side Surface :

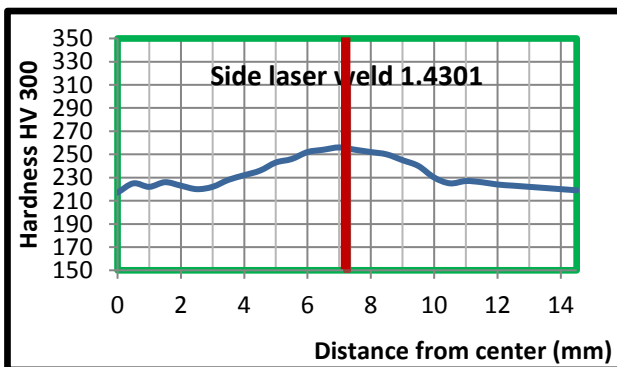


Figure 16 1.4301 A.S.S side surface laser weld hardness chart

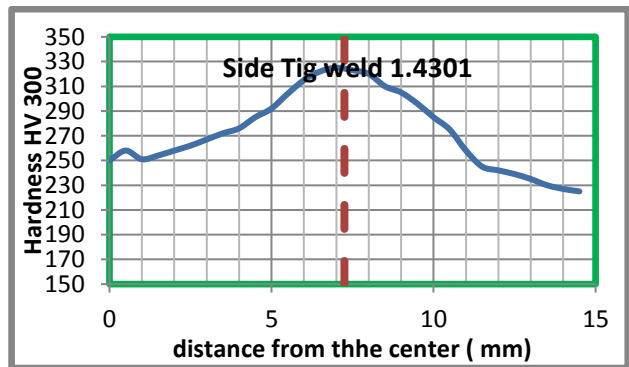


Figure 17 1.4301 A.S.S Side surface TIG weld hardness chart

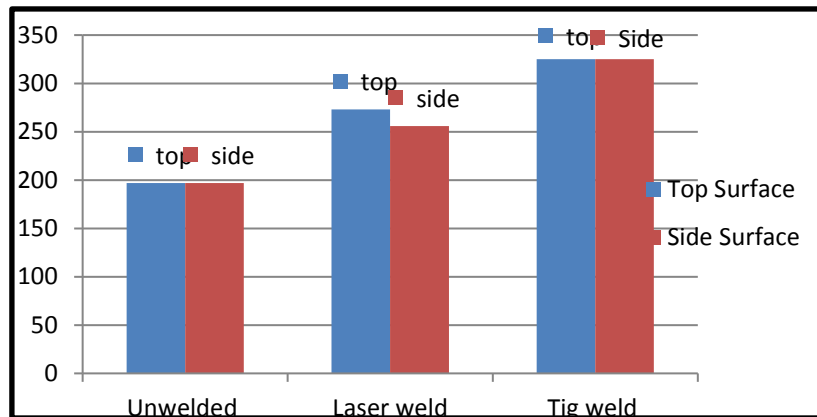


Figure 18-Histogram illustration for stainless steel 1.4301

3.5. Tensile testing:

Tensile strength testing was carried out for laser and Tig welding for comparison unwelded metal was used thickness 8mm. Observed that the weld done to the specimens done well compared to the original unwelded specimen that the tensile strength almost close to literature results (750 N/mm^2) fig.19. After several tests observed that the main reason about failing was some of the weld defects found in the weld zone that contain pores and cracks would weaken the material and can be affected by corrosion resulted in failure of the specimen below suspected breaking part. the incomplete penetration debilitates the material totally as the welding zone turns out to be not exactly the original measure. Compared to micro hardness measurement its assure that in the Tig weld its hardened which cause the failure at lower strength than Laser weld and the base metal. Through visual investigation of the tested specimens, the materials that performed best were the materials that had the least imperfections. In this manner, to choose which materials had the more exact welding conditions, we observe which specimens had the most elevated average ultimate strength.

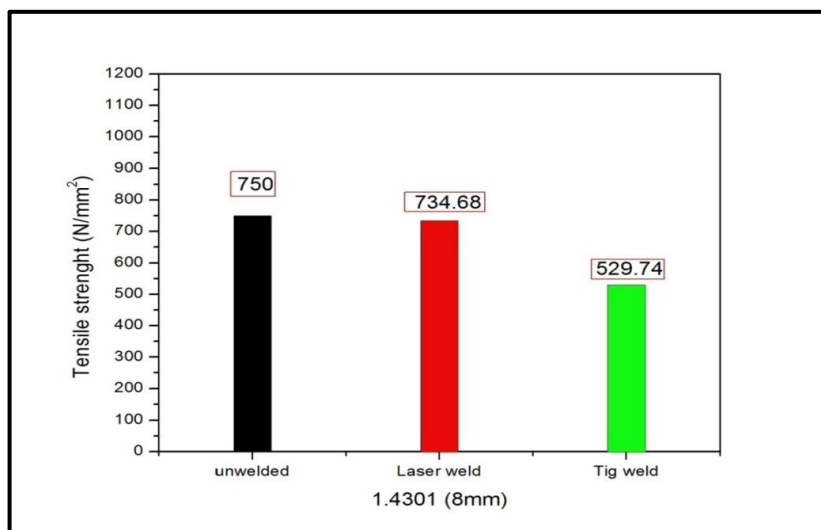


Figure 19 1.4301 A.S.S Tensile strength

3.6. Ferrite content

For the Stainless steel 1.4301 samples shown that during the probe passing across the specimen that the Ferrite % increased along moving across heat affected zone followed by the maximum in the weld zone which has lower corrosion resistant will be confirmed later in corrosion study happen due to the precipitate in the HAZ as found in figures (18 and 19) for top surfaces, figure (20 and 23) for side surfaces.

Ferrite distribution percent on the top surface:

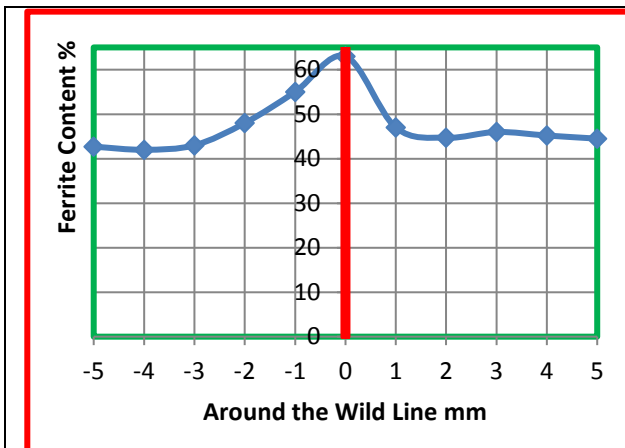


Figure 20- 1.4301 A.S.S ferrite % for top surface for Laser weld

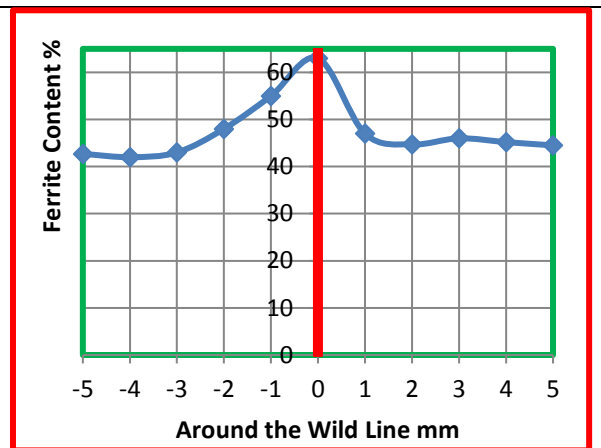


Figure 21 1.4301 A.S.S ferrite % Top Surface for TIG weld

Ferrite distribution percent on the side surface:

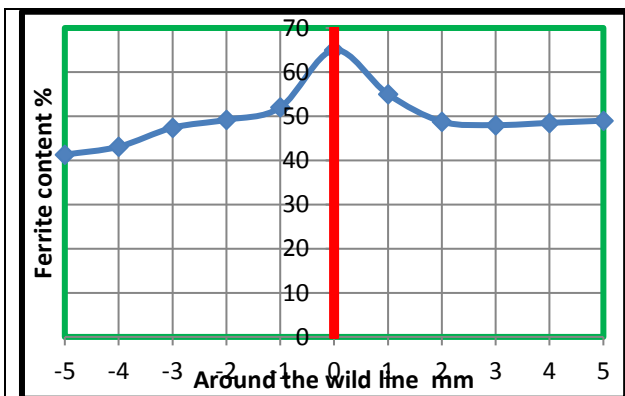


Figure 22-1.4301 A.S.S ferrite % for side surface for Laser weld

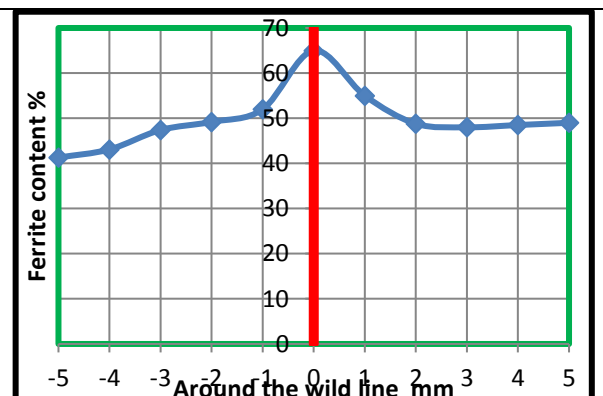


Figure 23-1.4301 A.S.S ferrite % Side Surface for TIG weld

**Electrochemical testing:
Open circuit potential (OCP):**

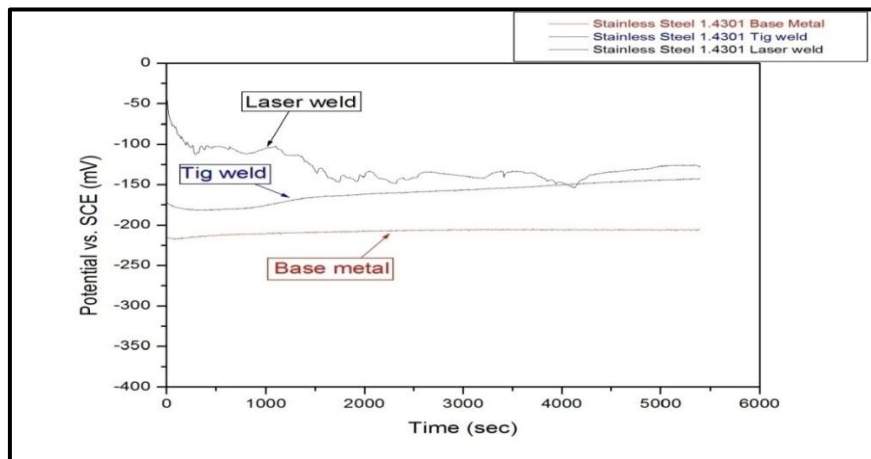


Figure 24- 1.4301 A.S.S OCP

In the above fig.24 in A.S.S 1.4301 the laser welded has a higher OCP values than the TIG welded and the Base metal (unwelded). Which illustrates that the welded material (Laser-Tig) has a higher passivity than the unwelded material in environment of 3.5% NaCl. At 4500sec (75mins) the laser -134.12mV compared to TIG which is -146.68mV the base metal(unwelded) is -205.68mV. As going from Laser welded specimen followed by the TIG welded specimen which indicates that the less negative potential direction is indication towards corrosion value happens due to the formation of carbides around the grain. The increase of potential from laser welds to TIG weld then the base metal may conclude laser re-passivation more corrosion resistant than TIG weld.

The open-circuit potential (OCP) give an indication about the dynamic behavior of the passive oxide layer film, whereas the more positive value for the OCP, the more the material becomes noble and corrosion resistant.

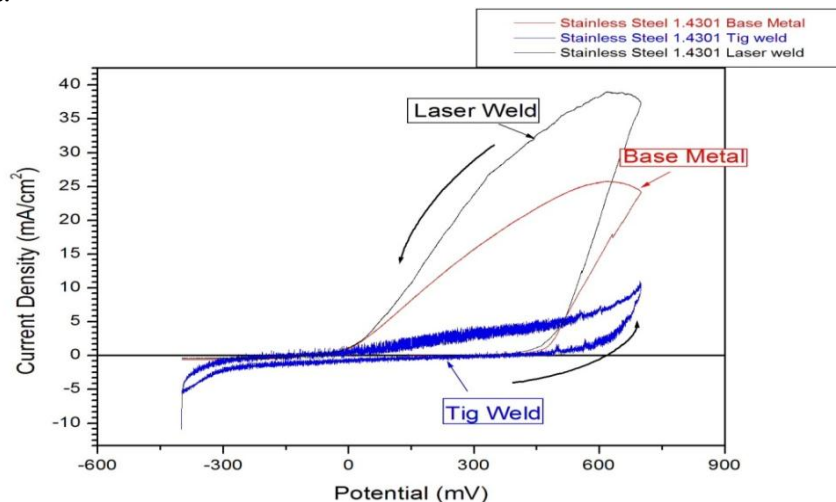


Figure 25 1.4301 A.S.S PCV

Corrosion rate

After conducting the Potential cyclic voltammetry for scan rate 2mV/sec from -400mV to 700mV it was seen from fig.25 for the laser weld is more pitting resistant comparing it to the corrosion rate of laser 9.436 mm/Y to the Tig welded 8.895 mm/Y from table4.

Table4 Corrosion rate

Condition	Corrosion rate (mm/Y)	Epitting(mV)
Unwelded	11.3	370
Laser weld	9.436	452.25
Tig weld	8.895	558.75

4. Conclusion

Optical microscopy reveals in showing that 1.4301 A.S.S undergoes type A solidification and also in grain refinement as the size of the grain much bigger in the base metal going to the HAZ and then in the weld zone which results in grain growth and elongated through the HAZ observing the increase in the ferrite content becomes the primary phase. There is many Weld defects seen under the microscope which decreased the strength and suspected region for the corrosion attack that need to overcome to result in the good weld and avoid these defects: porosity, incomplete fusion and cracks. Scanning electron microscopy revealed the precipitates at the grain boundaries of the weld line between the weld zone and heat affected zone (HAZ) followed by EDX test to track the Ni,Cr elements composition in the weld zone and out in HAZ and base metal. Micro hardness test processed on the top surface and the side surface to compare the diffusion of weld inside the whole material reveals seen increasing gradually from the base metal to the HAZ and then maximum at the weld zone in the center of weld. Found that the Tig weld and laser weld in both the side and top surface is higher than the base metal. Ferrite content represented the lower corrosion resistant at the weld zones which reached its maximum. Tensile test revealed that the welded specimen for A.S.S 1.4301 which welded by remote Scanner laser is almost the same as the base metal 734.68 N/mm² and 750 N/mm² respectively followed by the Tig weld 529.74 N/mm². Corrosion potential is higher in the welded materials (Laser-Tig) than the base metal in 1.4301 A.S.S. as Shown in OCP the welded materials (Laser-Tig). Pitting corrosion is observed.

It is recommended for the work to improve the welding procedure with different forms of weld joints considering all the above-mentioned parameters that affect the laser weld quality.

References

- [1] Norrish J. Advanced welding processes. Bristol: Springer Publishing; 1992.
- [2] Heubner, U. Nickel alloys. New York,USA: Dekker,ISBN:0-8247-0440-1,page(240-287). 2000
- [3] Steel products Manual: Stainless steel, Iron and Steel Society, U.S.A. : Warrendale. 1999
- [4] Callister Jr.,W.D.(2000), Fundamentals of Materials Science and Engineering, 5th Edition, U.S.A.: John Wiley & Sons,inc. 2005
- [5] J. Mazumder, Laser beam welding, ASM Handbook, vol. 6, 10th ed., Welding, Brazing, and Soldering, ASM International, Materials Park, OH, USA, 1990, pp. 263–268.
- [6] D. Schuocker, Welding with lasers, in: High Power Lasers in Production Engineering, Imperial College Press, UK, 1999, pp. 337–370.
- [7] David S.A. & Debroy T. (1992) Science 257 p.p. 497-502.
- [8] Steen, W.M. , Laser Material Processing, London: Springer-Verlag. 1991
- [9] Klotzbach, A.; Morgenthal, L.; Beyer, E.: Laser-beam welding with high speed beam deflection. Laser Opto 31(2)/1999. p.64.
- [10] Macken, J.: Remote Laser Welding. In: Proc. Of International Body Engineering Conference and Exposition, IBEC1996, Detroit (Mi), 1996.
- [11] Emmelmann, C.: Laserschweißen im Vielpunktwerkzeug für die Karosseriefertigung. Rofin Sinar. Hamburg, Sept. 1999.

- [12] Hornig, H.: Laserstrahlbearbeitung bei BMW: Anwendungen und Trends. In: Laserstrahlfügen: Prozesse, Systeme, Anwendungen, Trends. Hrsg.: Sepold, G.; Strahltechnik Band 19, BIAS Verlag, Bremen, Germany, 2002.
- [13] Marshall, P. Austenitic Stainless Steels: Microstructure and Mechanical Properties. London, NY: Elsevier. ISBN:978-0-85334-277-9, 1994.
- [14] Leopold, J. C. Welding metallurgy and weldability of stainless steels.chp.(6) Hoboken, NJ: John Wiley. ISBN:978-0-471-47379-4, 2005.
- [15] DIN Deutsches Institute für Normung e.v., DIN ISO 22826, Destructive tests on welds in metallic materials – Hardness testing of narrow joints welded by laser and electron beam (Vickers and Knoop hardness tests),(ISO 22826:2005), August 2008.
- [16] Holt J.M., Uniaxially tension testing, Vol.8: Mechanical testing and evaluation, ASM Handbook, ASM International, 2000.
- [17] Standard Practice for Steel Castings, Stainless, Instrument Calibration, for Estimating Ferrite Content, Designation: A 799/A799M – 92, (Reapproved 2002)
- [18] Kwok, C., Fong, S., Cheng, F., & Man, H. Pitting and galvanic corrosion behavior of laser-welded stainless steels. Journal of Materials Processing Technology,176(1-3), 168-178. doi:10.1016/j.jmatprotec.2006.03.128, 2006.
- [19] Jeffus, L. F., Welding principles and applications. Clifton Park, NY: Delmar Cengage Learning. Corrosion of Weldment (#05182G), 2012
- [20] Eid N.M., Localized corrosion at welds in structural steel under desalination plant conditions. Part I: Effect of surface roughness and type of welding electrode, Desalination, , Amsterdam 73 (1989) 397-406.
- [21] Weld integrity & performance, 2nd Edition, ASM International, U.S.A., 2001.
- [22] Lippold, J. & Kotecki, D. Welding Metallurgy and Weldability of Stainless Steels. New Jersey: John Wiley & Sons, inc. 2005.
- [23] N.A. McPherson, H. Samson, T.N. Baker, N. Suarez-Fernandez, Steel microstructure in autogenously laser welds, J. Laser Appl. 15, 2003